

# Input Shaper Design for Planar Parallel Manipulators

Madusudanan Sathia Narayanan  
PhD Candidate  
Department of Mechanical Engineering  
University at Buffalo (SUNY)  
Buffalo NY 14260 USA  
ms329@buffalo.edu

Venkat Krovi  
Associate Professor  
Department of Mechanical Engineering  
University at Buffalo (SUNY)  
Buffalo NY 14260 USA  
ms329@buffalo.edu

**Abstract**—The ever increasing demands on accuracy and faster response pose control challenges that are difficult to realize. Though advanced robust controllers can help address such demands to some extent, in reality actuator saturations and control limits can cause stabilized or sustained oscillations. In such scenarios, feed-forward methods and in particular input shaping (IS) seem to offer a valuable and cost-effective way for suppressing the residual vibrations [1] without major modifications to an existing system. Such schemes are found to be successful for a variety of (simple to complex) applications in flexible manipulators, gantry cranes etc [2], [3]. In this work, our focus is on the extending the traditional IS methods to constrained articulated multi-body systems (AMBS), specifically, for parallel manipulators (PMs) having revolute actuators. We present analytical formulation of linearized dynamic equations for a 5 bar (or 2-RR) and numerical computation of dominant mode frequency and eigenvalues of these systems. Dynamic simulation and IS control of the planar PM were subsequently carried out for simple point-to-point trajectory tracking problems. The corresponding results for shaped and unshaped inputs indicate considerable improvement in suppression of residual vibrations and were evaluated using reduction of maximum overshoot in position and torque inputs, settling time and percent residual energy as performance measures.

**Keywords** – parallel manipulators, input shaping, dynamic analysis, percent residual energy

## I. INTRODUCTION

The ever increasing demands on accuracy and faster response pose control challenges that are difficult to realize. Though advanced robust controllers can help address such demands to some extent, in reality actuator saturations and control limits can cause stabilized or sustained oscillations. The parasitic flexibilities, nonlinearities and multi-modal behaviors exhibited by a system present additional challenges for high precision applications. In such scenarios, feed-forward methods and in particular, one of the classical methods called input shaping (IS) [1] seem to offer a valuable and cost-effective way for suppressing the residual vibrations without major modifications to an existing system. This method relies on designing convolved inputs with

a chain of impulses with time-delays. Such schemes are found to be successful for a variety of (simple to complex) applications in flexible manipulators, gantry cranes etc [2], [3]. In this work, the focus is therefore on the applicability of IS methods to constrained articulated multi-body systems (AMBS), specifically, planar parallel manipulators (PMs) having revolute actuators.

## II. LITERATURE REVIEW

Singer and Seering [2] presented a simple, effective method that is now known as Impulse Input Shaping, which introduces a small time delay in a shaped reference trajectory. In short, the principle of input design, or input shaping, is to prevent the excitation of badly damped poles of a system by eliminating energy in the input signal at the specific frequencies corresponding to those poles. Impulse Input shaping produces zero residual vibration (as defined in [4], [5]) by creating a set of impulses with appropriate timing and amplitude, and convolving these impulses with the original reference trajectory. This effectively leads to the filtering of the specific frequencies from the input signal. The convolution of an impulse sequence with a reference trajectory in general shapes the entire trajectory for minimal residual vibration, which is not necessary for point to point motion.

Input shaping is basically employed for linear time invariant systems. It is beneficial especially when control performance requirements are not properly met in typical feedback control as well as open loop systems [6]. This can occur for various reasons including due to discrepancies between the simulated model and the actual system and due to contrasting design requirements indirectly imposed by limitations on actuators and controllers. In certain scenarios, robust shapers can be designed which can perform in presence of variations or uncertainties in the system parameters like natural frequencies. However, employing such a method for PM type nonlinear systems requires linearization of dynamic models.

So far, only a very few have succeeded in applying

IS method to suppress residual vibrations for trajectory tracking problems using PMs. Kozak et al [3] discuss a basic application of input shaping techniques for 2 DOF manipulators while the same had been applied for 3 DOF flexible linkage system in [7]. However, both these systems have prismatic actuators as active joints which simplify the kinematic and eventually dynamic models of the system compared to revolute actuators which is dealt in this paper.

### III. MATH BACKGROUND

#### A. Parallel Platform Manipulator Kinematics

In order to solve the systems of dynamic equations of motions (EoMs), it is first necessary to derive the system level position and velocity kinematic equations [8]. For a generic multi-link parallel platform manipulators (PPM), a PM having multiple serial chains attach at various points of a central platform, as in Fig. 1, the position of the central platform is of interest (task space control variable). In the Cartesian space, the platform position can be expressed using vector loop closure technique for a  $j^{th}$  chain as follows:

$$\mathbf{H}^j(\mathbf{q}) = \mathbf{O}\mathbf{A}_0^j + \mathbf{A}_0^j\mathbf{A}_1^j + \mathbf{A}_1^j\mathbf{A}_2^j + \dots + \mathbf{A}_{n_j-1}^j\mathbf{A}_{n_j}^j = \mathbf{O}\mathbf{X} \quad (1)$$

where,  $n_j$  is number of links in  $j^{th}$  chain (in this work,  $n_j = n$ ,  $\forall j = 1 \dots m$  chains), and  $(\mathbf{A}_k^j)_{k=1 \dots n-1}$  are end points (or joint centers) of links and  $\mathbf{A}_n^j$  are platform attachment points for  $j^{th}$  chain. Eqn.(1) is a nonlinear vector algebraic equation that are usually difficult to solve analytically.

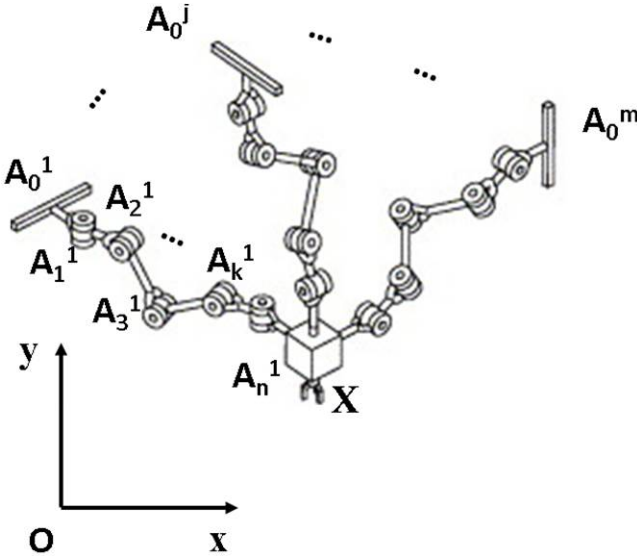


Fig. 1: Multi Chain Parallel Mechanism

For inverse kinematics it has to be solved for the joint or configuration coordinates,  $\{\mathbf{q} \equiv [\mathbf{q}_a^T \mathbf{q}_p^T]^T \in \mathbb{R}^N$ , where  $\mathbf{q}_a^T \in \mathbb{R}^{\tilde{N}}$  are the actuated joint coordinates,  $\mathbf{q}_p^T \in \mathbb{R}^{N'}$  are the passive joint coordinates and  $\tilde{N} + N' = N$  is the

dimension of total joint space}, given the Cartesian position and orientation of the central link/ platform,  $\mathbf{X} \in \mathbb{R}^M$ . For the case of PPMs, several nonlinear analytical formulations exist such as Freudenstein's or intersection of circles and a detailed survey of these methods can be found in [8]. On the contrary, given the complete joint configuration of such systems (LHS of eqn.(1)), forward kinematics to determine the platform configuration (RHS of eqn.(1)) is straightforward, even for spatial complex systems, provided complete configuration (both passive and active joint angles) is known or can be computed. It is noted that depending upon the values of  $N, \tilde{N}, N'$  and  $M$ , any AMBS system can be categorized into under-actuated ( $\tilde{N} < M$ ), kinematically redundant ( $N > M$ ), fully-actuated ( $\tilde{N} = M$ ) and redundantly actuated systems ( $\tilde{N} > M$ ). In this work, however, we will only focus on fully actuated PPMs for which  $\tilde{N} = M$ .

Differentiating eqn.(1) w.r.t. time ( $t$ ) yields the velocity level kinematic equations for each chain which in turn can be simplified further to obtain the respective link and platform Jacobian matrices.

$$\dot{\mathbf{V}}_{\mathbf{x}} = \frac{\partial \mathbf{H}^j(\mathbf{q})}{\partial \mathbf{q}} \dot{\mathbf{q}} = \mathbf{J}_p^j \dot{\mathbf{q}} \quad (2)$$

where,  $\mathbf{H} \equiv [\mathbf{H}^j]_{j=1 \dots m}$ ,  $\dot{\mathbf{V}}_{\mathbf{x}} \in \mathbb{R}^M \equiv$  platform end effector velocity and  $\mathbf{J}_p^j \in \mathbb{R}^{M \times N} \equiv$  link Jacobian matrices for each chain. The link Jacobian matrix,  $\mathbf{J}_p^j$  linearly relates the end effector velocity,  $\dot{\mathbf{V}}_{\mathbf{x}}$  to joint rates  $\dot{\mathbf{q}}$  and the platform Jacobian matrix ( $\mathbf{J}_p \in \mathbb{R}^{M \times N}$ ) can be obtained by collecting the rows of  $\mathbf{J}_p^j$  corresponding to the actuated joint rates,  $\dot{\mathbf{q}}_a$ .

#### B. Constraint Velocity Matrix

In this work, we intend to use augmented Lagrangian method (ALM) as in eqn.(5) to derive the final EoMs in terms of extended joint coordinates. This is achieved by splitting up the complete PPM as in Fig.1 into individual chains except for one chain (say for the chain,  $j = 1$ ) to which the central platform is included as the end link. So, the EoMs of the PPM having  $M$  degrees of freedom (DOF) in task-space will be parameterized using the entire joint coordinates (assuming all joints to be 1-DOF except platform attachment joint) having a total of  $n \times m + \tilde{m}$  or  $N + \tilde{m}$  DOF, i.e. ( $n$  DOF joints per chain  $\times m$  chains  $+\tilde{m}$  DOF to account for the joint attachment between central platform to the penultimate link of the 1st chain, and total joint coordinates,  $N = n.m$ ). So, by this approach we end up with  $(N + \tilde{m})$  number of EoMs, requiring  $(N + \tilde{m}) - M$  independent constraint velocity equations for ALM. The total joint coordinate vector,  $\mathbf{q}$  will now be extended using the additional  $\tilde{m}$  DOF, i.e.  $\mathbf{q} \in \mathbb{R}^{N+\tilde{m}}$ . For example, a 2-RR mechanism as in Fig.3 has  $n = 2$  links per chain,  $m = 2$  chains,  $M = 2$  ( $x_e, y_e$ ). Therefore, number of constraint equations, assuming all joints to be 1 DOF and the central platform to be a point mass attached to the end of the 1st chain (which does not contribute to any additional

DOFs, i.e.  $\tilde{m} = 0$ ), will be:  $N + 0 - M = 4 - 2 = 2$ , thereby requiring us to find two velocity level constraints from vector loop closure equations. These position-level-constraint equations are iteratively obtained from Eqn.(1) for two successive chains as follows, which provided us a simpler way of obtaining the desired number of constraints eliminating the task space variables ( $\mathbf{X}$ ) altogether:

$$\begin{aligned} \mathbf{C}^j(\mathbf{q}) &= \mathbf{H}^{j+1} - \mathbf{H}^j = 0 \\ \Rightarrow \mathbf{C}(\mathbf{q}) &= [\mathbf{C}^j(\mathbf{q})]_{j=1}^{m-1} = 0 \end{aligned} \quad (3)$$

Eqn.(3) is only one scheme of generating independent constraint equations and there are usually numerous ways to find required number of constraint equations as long as all of those are independent with each other.

Differentiating eqn.(3) w.r.t.  $t$  yields the velocity level constraint equation as:

$$\frac{\partial \mathbf{C}(\mathbf{q})}{\partial \mathbf{q}} \frac{\partial \mathbf{q}}{\partial t} = 0 \Rightarrow \mathbf{B}(\mathbf{q}) = \frac{\partial \mathbf{C}(\mathbf{q})}{\partial \mathbf{q}} \Rightarrow \mathbf{B}(\mathbf{q}) \frac{\partial \mathbf{q}}{\partial t} = 0 \quad (4)$$

where  $\mathbf{B}(\mathbf{q}) \in \mathbb{R}^{(N-M) \times N}$  will be used in Lagrangian EoMs as explained in the next section.

### C. Constrained Lagrangian Formulation for Parallel Manipulators

With positions and velocities of mass centers of all the links expressed in terms of joint coordinates  $\mathbf{q}$  and the corresponding rates  $\dot{\mathbf{q}}$ , individual kinetic ( $\mathbf{T}$ ) and potential ( $\mathbf{V}$ ) energies and eventually, system Lagrangian ( $\mathbf{L}$ ) can be readily calculated as  $\mathbf{L} = \mathbf{T} - \mathbf{V}$ . Using the system Lagrangian,  $\mathbf{L}$ , the final EoMs can be obtained using ALM as:

$$\frac{d}{dt} \frac{\partial \mathbf{L}}{\partial \dot{q}_i} - \frac{\partial \mathbf{L}}{\partial q_i} \frac{\partial \Pi}{\partial \dot{q}_i} - \frac{\partial \Delta}{\partial \dot{q}_i} - \sum_{k=1}^{(N+\tilde{m})-M} \frac{\partial \mathbf{C}_k}{\partial q_i} \lambda_k, \quad \forall i = 1 \dots (N + \tilde{m}) \quad (5)$$

where  $\mathbf{C}_k$  is the  $k^{th}$  row of equation from eqn.(3),  $\Pi$  and  $\Delta$  are sum of all external inputs and dissipation elements of the system respectively and  $\lambda = (\lambda_k)_{k=1 \dots (N+\tilde{m}-M)}$ . A detailed discussion on this method can be found in [8].

Simplifying eqn. (5) and combining the joint rates and accelerations terms together, the final dynamic equations of motion (EoM) for a typical PPM in Fig. 1 takes the form of 2nd-order differential algebraic equations as:

$$\begin{aligned} \mathbf{M}(\mathbf{q}, \dot{\mathbf{q}}) \ddot{\mathbf{q}} + \mathbf{N}(\mathbf{q}, \dot{\mathbf{q}}) + \mathbf{G}(\mathbf{q}) &= \boldsymbol{\tau} - \mathbf{B}^T \boldsymbol{\lambda} \\ \mathbf{B}(\mathbf{q}) &= \frac{\partial \mathbf{C}(\mathbf{q})}{\partial \mathbf{q}} \end{aligned} \quad (6)$$

where mass matrix ( $\mathbf{M}$ ), centrifugal and Coriolis vector ( $\mathbf{N}$ ), gravitational vector ( $\mathbf{G}$ ) and input torques ( $\boldsymbol{\tau}$ ) are used. The corresponding derived matrices for 2-RR manipulator is given in the appendix A in eqns. (14) and (17).

The feedback loop is implemented to simulate simple point-to-point trajectory tracking problems. A simple

proportional derivative (PD) control is considered in this work for which the control torques can be computed as  $\boldsymbol{\tau} = \mathbf{K}_P(\mathbf{q}_{des} - \mathbf{q}_{curr}) + \mathbf{K}_D(\dot{\mathbf{q}}_{des} - \dot{\mathbf{q}}_{curr})$ .  $\mathbf{K}_P$  and  $\mathbf{K}_D$  are typically diagonal matrices with values representing control gains in joint-space, i.e.  $\mathbf{K}_P = \text{diag}([k_{p,i}]_{i=1}^n)$  and  $\mathbf{K}_D = \text{diag}([k_{d,i}]_{i=1}^n)$ .  $\mathbf{q}_{des}$  and  $\mathbf{q}_{curr}$  represent the desired and current joint trajectories. For the sake of implementation of IS control, the control gains need to be tuned to be able to generate stable or conditionally stable tracking of trajectories.

### D. Frequency and damping ratio distribution

Studying the frequency characteristics of nonlinear systems and determining the poles for such systems are extremely difficult, if not impossible. It is therefore necessary to linearize the dynamic model in eqn.(6) about the equilibrium point,  $\mathbf{q}_0$  of the configuration space, assuming negligible joint velocities and neglecting non-linear terms,  $\mathbf{N}(\mathbf{q}, \dot{\mathbf{q}})$ , to get:

$$\tilde{\mathbf{M}}(\mathbf{q}_0) \Delta \ddot{\mathbf{q}} + \tilde{\mathbf{C}} \Delta \dot{\mathbf{q}} + \tilde{\mathbf{K}} \Delta \mathbf{q} + \tilde{\mathbf{B}}^T(\mathbf{q}_0) \tilde{\boldsymbol{\lambda}} = \mathbf{0} \quad (7)$$

Diff. eqn.(4) and linearizing about  $\mathbf{q}_0$ , we get:

$$\begin{aligned} \tilde{\mathbf{B}}(\mathbf{q}_0) \Delta \ddot{\mathbf{q}} + \dot{\tilde{\mathbf{B}}}(\mathbf{q}_0) \Delta \dot{\mathbf{q}} &= \mathbf{0} \\ \tilde{\mathbf{B}}(\mathbf{q}_0) \Delta \dot{\mathbf{q}} &= -\dot{\tilde{\mathbf{B}}}(\mathbf{q}_0) \Delta \dot{\mathbf{q}} \end{aligned} \quad (8)$$

where,  $\Delta \mathbf{q}$ ,  $\Delta \dot{\mathbf{q}}$  and  $\Delta \ddot{\mathbf{q}}$  are finite differences and their derivatives between the operating point and the actual point;  $\tilde{\mathbf{K}} = \text{diag}([k_{p,i}]_{i=1}^n) = \mathbf{K}_P$  and  $\tilde{\mathbf{C}} = \text{diag}([k_{d,i}]_{i=1}^n) = \mathbf{K}_D$ .  $\tilde{\mathbf{M}}$  is the linearized mass matrix =  $\mathbf{M}|_{\mathbf{q}=\mathbf{q}_0}$ . Combining eqns. (7) and (8), we get:

$$\begin{aligned} \underbrace{\begin{Bmatrix} \tilde{\mathbf{M}} & \mathbf{0} \\ \mathbf{0} & \mathbf{0} \end{Bmatrix}}_{\mathbf{M}_s} \underbrace{\begin{Bmatrix} \Delta \ddot{\mathbf{q}} \\ \Delta \tilde{\boldsymbol{\lambda}} \end{Bmatrix}}_{\Delta \ddot{\mathbf{p}}} + \underbrace{\begin{Bmatrix} \tilde{\mathbf{C}} & \mathbf{0} \\ \mathbf{0} & \mathbf{0} \end{Bmatrix}}_{\mathbf{C}_s} \underbrace{\begin{Bmatrix} \Delta \dot{\mathbf{q}} \\ \Delta \tilde{\boldsymbol{\lambda}} \end{Bmatrix}}_{\Delta \dot{\mathbf{p}}} + \dots \\ \underbrace{\begin{Bmatrix} \tilde{\mathbf{K}} & -\tilde{\mathbf{B}}^T \\ \tilde{\mathbf{B}} & \mathbf{0} \end{Bmatrix}}_{\mathbf{K}_s} \underbrace{\begin{Bmatrix} \Delta \mathbf{q} \\ \Delta \tilde{\boldsymbol{\lambda}} \end{Bmatrix}}_{\Delta \mathbf{p}} = \mathbf{0} \end{aligned} \quad (9)$$

As it can be seen in eqns. (7) and (9), the linearized model becomes a multi-pole second order system using which the natural frequencies and damping ratios of the system could be determined. This is done by using the characteristic equation (CE) obtained by taking the Laplace transform of eqn.(9) as:

$$\tilde{\mathbf{M}}_s s^2 + \tilde{\mathbf{C}}_s s + \tilde{\mathbf{K}}_s = \mathbf{0} \quad (10)$$

The corresponding poles of eqn.(10) is used to obtain natural frequency and damping ratio to design our input shapers. Depending on the extent of nonlinearity of the system, these quantities tend to vary widely within the desirable work volume.

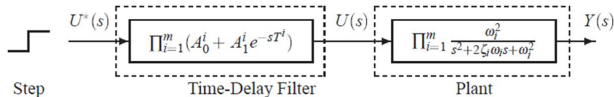


**Fig. 2:** Multi-Mode Standard Time Delay Input Shaper Control [6]

### E. Input Shaper (IS) Design

IS are generally characterized by their step or impulse amplitudes ( $A_i$ ) and their corresponding time-delays ( $T_i$ ). Analytical expressions of standard IS parameters for a second order system have been derived in [2] (based on natural frequency,  $\omega_i$  and damping ratios,  $\zeta_i$  of  $i^{th}$  dominant pole of a typical multi-pole linear system). Safely assuming the linearity of the system, these values can be obtained from the location of the respective dominant pole ( $\alpha_i \pm j\beta_i$ , where  $j = \sqrt{-1}$ ). The derived parameters for a standard 2-step input shaper ( $A_1, A_2, t_1, t_2$ ) for  $i^{th}$  pole ( $\alpha_i \pm j\beta_i \equiv \zeta_i\omega_i \pm \omega_i\sqrt{1-\zeta_i^2}$ ) are given by:

$$\begin{aligned} K &= e^{-\frac{\zeta_i\pi}{\sqrt{1-\zeta_i^2}}} \\ T_0 &= 0, T_1 = \frac{\zeta_i\pi}{\sqrt{1-\zeta_i^2}} \\ A_0 &= \frac{K}{1+K}, A_1 = \frac{1}{1+K} \end{aligned} \quad (11)$$

In order to ensure the output is consistent with the input magnitude, the amplitudes,  $A_j^i$ , for  $i$ -th pole in eqn.(12) are normalized to one ( $\sum_j A_j^i = 1, A_j^i \geq 0, \forall j$ ). A general multi-pole multi-step input shaper cascaded with a 2nd order dynamic system is represented in block form in Fig.2 by principle of linear superposition of IS. For multi-pole systems, the IS parameters are determined for each dominant pole and cascaded in series to progressively split a single step input into sequence of smaller step inputs and feed into the system as in Fig. 2.

## IV. SYSTEM DEFINITION

In this work, we consider the simplest fully-actuated symmetric PPM, namely 2-RR manipulator (or a five bar mechanism with central point mass located at the point where the end effectors of both the arms meet) as shown in the Fig. 3 for which  $\tilde{N} = M$ . The Rs in the names of the PPM stand for the revolute joints (in general, P stands for prismatic, C for cylindrical, U- universal and S for spherical joints) in each arm of the manipulator, while the underline indicates the actuated joints. The word symmetric here implies that not only the number of links in each chain but also the joint arrangements for each chain of the PPM are same. In addition, the PPMs are assumed to operate in a horizontal plane so that the effects due to gravitational forces including the term,  $\mathbf{G}(\mathbf{q})$  shall be neglected hereafter from eqn.(6). However, it is noted that the method can be generalized to any type of systems that violate these assumptions (including out-of-plane or spatial

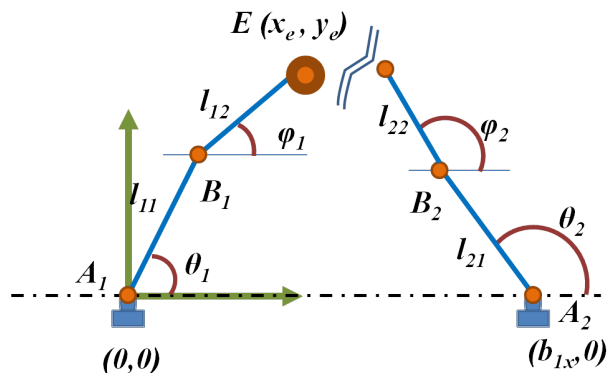


**Fig. 3:** 2-RR Parallel Manipulators (split at E):  $I_{i,1} = 0.04$ ,  $I_{i,2} = 0.12$ ,  $I_p = 0.082$ ,  $m_{i,j} = 0.1$ ,  $m_p = 0.5$ ,  $b_{1_x} = 1$

robots and redundant manipulators) as long as the underlying kinematic equations are solvable. Such complex systems will be considered as a part of our future efforts.

The schematic of the system is shown in the Fig. 3 using the values of the geometric and dynamic parameters as listed in Table.I for our simulations. The resulting forward dynamic models of the 2-RR manipulator and the control implementations were carried out within MATLAB-Simulink using a fixed step solver (ode3) and a step size of 0.0001 seconds as shown in the Fig.4. It comprises of a feedback PD controller with proportional and differential gain matrices,  $K_P$  and  $K_D$  respectively encapsulated within input control block. Using eqn.(10), the distributions of  $\omega_i$  and  $\zeta_i$  corresponding to the dominant pole(s) were determined to design our IS as per the eqns.(12). The distributions of natural frequencies and damping ratios for the linearized dynamic model of 2-RR system corresponding to the dominant pole are shown in Fig. 5. The variations in damping ratios are similar (while magnitudes are different however) to the corresponding natural frequencies and hence, only the frequency plots are shown here.

## V. RESULTS

### A. Unshaped Response

Prior to proceeding with IS design, it is necessary to guarantee the stability (or at the least, conditional stability) of the dynamic system with or without a feedback control (in our case, we chose PD control) for trajectory tracking. The IS enables one to only modulate the control inputs and does not affect or change the stability characteristics of the dynamic system. So, the PD control gains are first tuned to satisfy this condition and the unshaped responses of the PPM are obtained. This response is overlaid on all the plots of system responses (input positions and torques) to provide a visual comparison for achieved improvement due to IS.

### B. Shaped Responses

A series of input shapers can then be designed not only for position-level point-to-point (P2P) and multi-step (Mu-

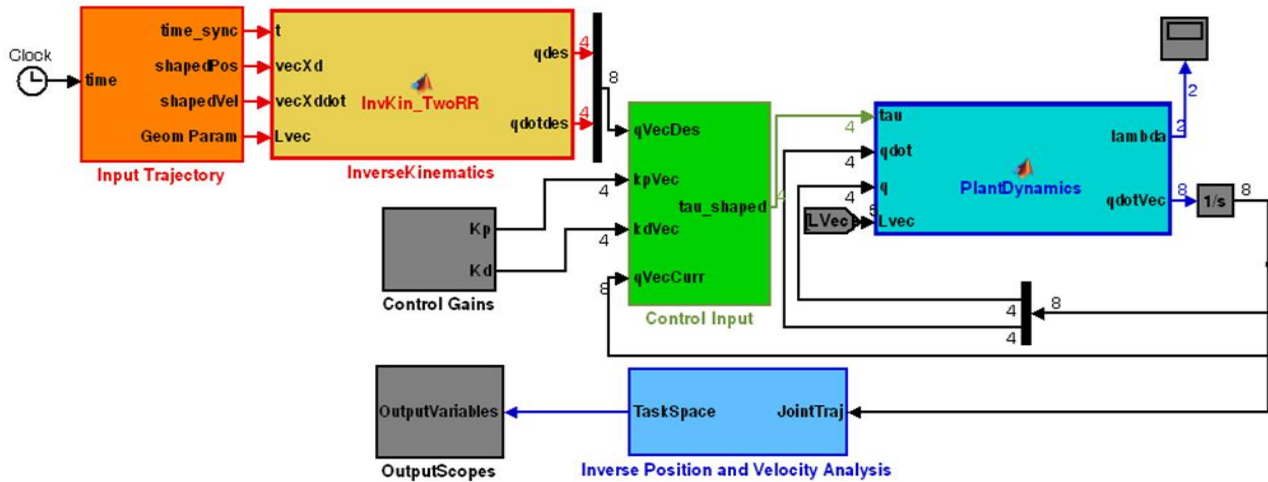


Fig. 4: Simulink Implementation for PD Control and Input Shaping of PM

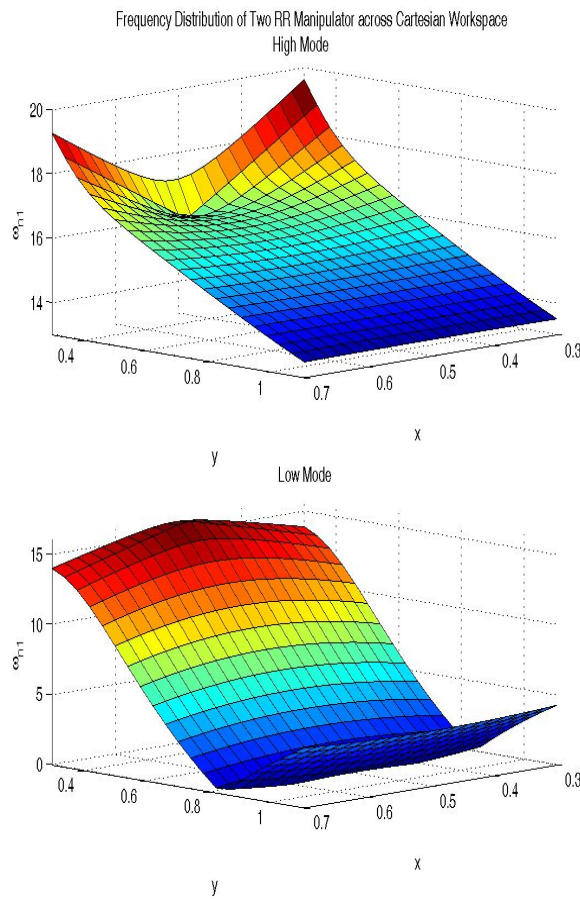


Fig. 5: Frequency Distribution of 2 – RR Manipulators

St) maneuvers but also for desirable task space velocity profiles. In the case of velocity-level control, the desired positional inputs are obtained by integrating the velocity profiles (for example, integral of unit step is unit ramp) and the input shaper coefficients remain the same as earlier but now acts on the integrated input (ramp in this case) of the system. Though extensive set of case studies were tested and analyzed, only a subset of these (P2P and Mu-St trajectory tracking case studies) are discussed here to understand the resulting benefits.

Specifically the following set of desired trajectories were used and the corresponding input shaper controls were examined. Since the start and end states of system are well defined for P2P maneuvers, that information could be used to analytically design input shapers offline using eqns.10 and 12. However, the values obtained by this method are limited by the use of the linearized model used to compute the dominant poles. Nonetheless this satisfies our desired response characteristics in this work. The following list indicates different trajectory testing case-studies carried out.

- Trajectory A: (0.5, 0.5) to (0.5, 0.6)
- Trajectory B: (0.6, 1.15) to (0.7, 1.15)
- Trajectory C: (0.2, 0.6) to (0.5, 1.15)

The IS performance were evaluated by computing the system frequencies at start-, end- and middle- points of the trajectory. Figure 6 shows the system response and control inputs after shaping only using the mean-value shaper (i.e. shaper parameters obtained by using the center-point of the task-space trajectory of the end-effector platform). The symbols in the legend (UnR, Sh, Sl, Multi) of Fig. 6 corresponds to (unshaped, high-frequency mode compensated, low frequency mode compensated and multi mode compensated responses) of the system respectively.

**TABLE I:** List of Kinematic and Geometric Parameters

Sym.	Description	Values	Units
$J_{i,j}$	Moment of inertia of the link, $i$ in chain, $j$	$I_{i,1} = 0.04$ , $I_{i,2} = 0.12$	$kg.m^2$
$l_{i,j}$	Length of link $i$ in chain, $j$	0.2	$m$
$lc_{i,j}$	Location of mass center of link $i$ in chain, $j$ from the $(i-1)^{th}$ joint center	0.1	$m$
$\lambda$	Constraint forces or Lagrange multipliers		$N$
$l_p$	Platform side length	0.04	$m$
<b>B</b>	Velocity level constraint matrix (obtained from loop closure equations)		–
$m_{i,j}$	Mass of the link $i$ in chain, $j$	0.1	$kg$
$m_e$	Mass and inertia of central platform	0.5	$kg$
$b_{jx}, b_{jy}$	Base joint location for $j^{th}$ chain	$j = 1 : [1, 0]^T$ , $j = 2 : [0.5, 0.87]^T$	$m$
<b>Joint Coordinates (Active and Passive)</b>			
$\theta_j$	Active revolute joint in each chain (j)		rad
$\phi_j$	Passive revolute in each chain $j$		rad

The model responses were recorded for each test trajectory and each input-shaping type (high, low and multi mode compensated). It can be clearly seen for this specific case that the damped oscillations in the system are suppressed compared to the unshaped response resulting in desirable characteristics (reduced overshoot, faster settling time and reduced torque magnitudes) for the platform.

The trajectories used in general lie in different regions of the workspace and enables to understand the feasibility of our method for manipulators describing local motions (length of each trajectory is considered to be small) around distant points within the workspace. The main reason to intentionally choose such trajectories is to avoid unnecessary complications induced by wide variation in natural frequencies and damping ratios which is a severe limiting factor that will be addressed in future work. The test trajectory, C, however, covers a larger workspace from its center to near the boundaries of desirable operating region. Implementing standard IS control may lead to undesirable oscillations and even result in worse performance than the unshaped responses. In order to extend the IS to such applications, we implement Mu-St based IS control. This implies that when the desired trajectories traverse larger regions of the

workspace, it is possible to compound the single P2P maneuver to multiple close-spaced P2P trajectories. The system response plot for this case was implemented using only the MVS on two compounded step inputs to the system as shown in Fig. 7.

The performance improvement of IS for P2P trajectory maneuverable problems in comparison to unshaped responses were evaluated using some standard metrics such as percent residual vibration ( $PRV$ ), settling time ( $T_s$ ) and maximum overshoot ( $M_p$ ) that are commonly used for linear systems and discussed in detail in Kozak et al. [9]. Since the systems considered in this work are nonlinear, multi DOF and multi-modal, only three measures were considered to be useful: fixed and zero times-based maximum overshoot in position ( $M_p^{q_i}$  and  $M_p^{q_i}(t_s)$ ) and control torques ( $M_p^{\tau_i}$  and  $M_p^{\tau_i}(t_s)$ ) respectively, settling time ( $T_s$ ) and percent residual energy ( $PRE$ ). For our systems,  $PRE$  were calculated as kinetic energies at the corresponding settling time for each control mode,  $\sum_{i=1}^{\tilde{N}} \tau_i \dot{\theta}_i^2$  as potential energy terms are zero.

The use of  $M_p^{\tau_i}$  on torque inputs is emphasized in our work as these directly determine the maximum actuator capacities. In a way it indicates a quantitative measure of how much the IS can help overcome maximum actuator limits while at the same time providing desirable response characteristics. It can also be easily observed from the response plots of our case studies that  $M_p^{\tau_i}(t_s)$  and  $M_p^{\tau_i}(t=0)$  turn out to be a more conservative estimate than the percentage ratios of shaped and unshaped input torque overshoots. The Table II summarizes the response characteristics of IS in terms of the aforementioned performance measures.

From this tabulation, we see that even though vibration suppression is guaranteed by the IS, ensuring the same w.r.t. actuator inputs is not possible which would require a more detailed analysis that is outside the scope of the current work. This limitation is mainly due to the underlying system complexities (nonlinear, multimodal and multi-DOF) which affects the modal characteristics of the system and in turn, compromises the trajectory tracking capability. Therefore energy based measures, such as percent residual energy ( $PRE$ ) should be preferred to any other measures that can capture the vibration suppression effects in a more generalized and conservative manner.

## VI. DISCUSSION

Thus, we were able demonstrate the applicability and viability of input shaping techniques to PPMs with preliminary results for a specific case of  $2 - \underline{RR}$  system. The resulting platform trajectories and actuator efforts were then evaluated using standard performance measures discussed in [9] such as % rise/ decrease in  $M_p$  of positions and actuated torques, and % residual energy ( $PRE$ ). Our future efforts will focus on extending this to PPMs with orientational DOF (such as  $3 - \underline{RRR}$ ,  $3 - \underline{RPR}$ ,  $3 - \underline{PRR}$  etc) and complex spatial PPMs (SPMs). We also intend to apply these techniques to SPMs,

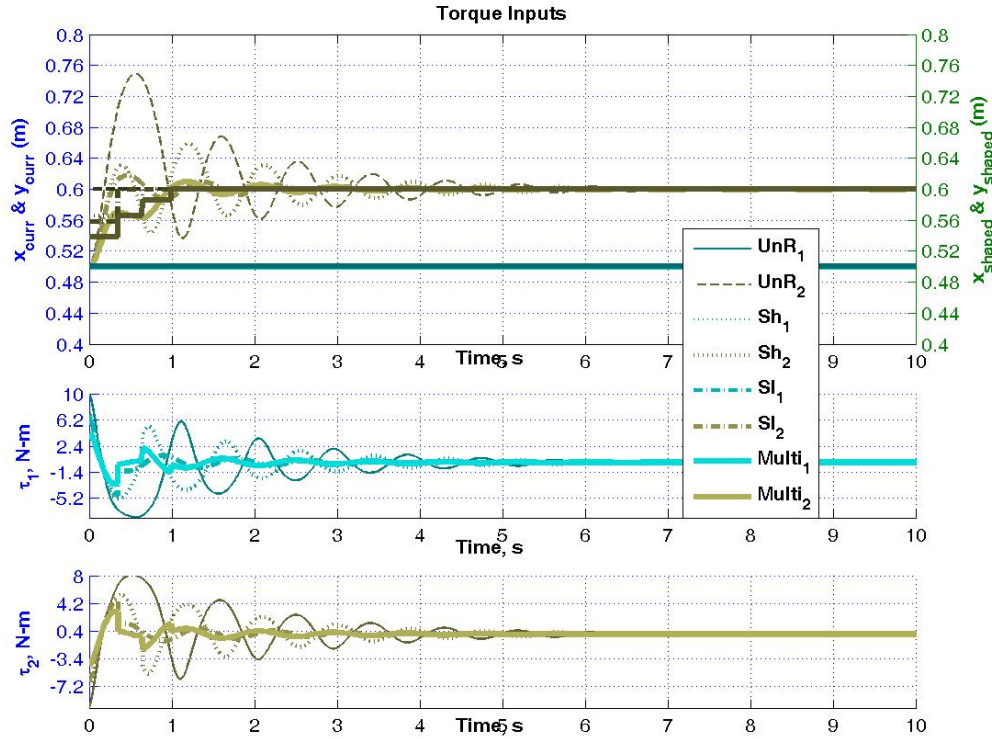


**Fig. 6:** Unshaped and Shaped Responses and Torque Inputs of 2 –  $RR$  PPM based on Mean Value Shaper ( $\%M_p$  in pos:(0, 39.1),  $\%M_p$  in actuated torques: (0, 8.3) and  $PRE$  at settling time: 1.4)

**TABLE II:** Evaluation of IS for 2 –  $RR$  Manipulators

	$\% \frac{M_p(t=0)^{sh}}{M_p(t=0)^{un}}$	$\% \frac{T_s^{un} - T_s^{sh}}{T_s^{un}}$	$\%M_p^{\tau_i}$	PRE
IVS(A)-H	0,39.6	0, 8.3	74.1,75.7	1.5
IVS(A)-M	0,11.1	0,46.0	71.8,72.2	0.0
MVS(A)-H	0,39.1	0,8.3	74.1,75.6	1.4
MVS(A)-M	0, 6.6	0,59.6	71.8,72.1	0.0
FVS(A)-H	0,38.2	0,8.5	74.1,75.6	1.5
FVS(A)-M	0,13.7	0,40.7	69.0,67.6	0.1
MVS(B)-M	15.8,0	47.2,0	92.1,109.3	4.6
MVS(C)-H	15.5,18.2	33.7,41.2	53.2,72.1	6.3

Unshaped response torque overshoot: Traj A (79.1, 80.6), Traj B (76.0,89.4), Traj C-1st step: (131.3,110.1) & Traj C-2nd step (92.7,88.7); (H: High mode and M: Multi mode IS control)

especially 5-DOF High-definition haptic device ( $HD^2$ ) [10] and 6-DOF hexapod [11] for vibration-free pose tracking and force feedback applications. Additionally, evaluating the robustness of the IS to parametric uncertainties will be more useful for such practical applications.

#### REFERENCES

- [1] N. C. Singer and W. P. Seering, "Artificial intelligence at mit," P. H. Winston and S. A. Shellard, Eds. Cambridge, MA, USA: MIT Press, 1990, ch. Preshaping command inputs to reduce system vibration, pp. 128–147.

- [2] W. Singhose, B. Mills, and W. Seering, "Vibration reduction with specified swing input shapers," in *International Conference on Control Applications*, vol. 1, 1999, pp. 533–538.
- [3] K. Kozak, I. Ebert-Uphoff, and W. Singhose, "Locally linearized dynamic analysis of parallel manipulators and application of input shaping to reduce vibrations," *Journal of Mechanical Design*, vol. 126, no. 1, pp. 156–168, 2004.
- [4] J. Vaughan, A. Yano, and W. Singhose, "Comparison of robust input shapers," *Journal of Sound and Vibration*, vol. 315, no. 4–5, pp. 797–815, 2008.
- [5] W. Singhose, W. Steering, and N. Singer, "Residual vibration reduction using vector diagrams to generate shaped inputs," *Journal of Mechanical Design*, vol. 116, no. 2, pp. 654–659, 1994.
- [6] T. Singh, *Optimal Reference Shaping for Dynamical Systems: Theory and Applications*, 3rd ed., G. Salvendy, Ed. John Wiley & Sons, 2010.
- [7] L. Bing, Z. Xuping, J. K. Mills, W. L. Cleghorn, and X. Liyang, "Vibration suppression of a 3-prr flexible parallel manipulator using input shaping," in *International Conference on Mechatronics and Automation (ICMA)*, 2009, pp. 3539–3544.
- [8] L.-W. Tsai, *Robot Analysis : the mechanics of serial and parallel manipulators*. John Wiley & Sons, 1999.
- [9] K. Kozak, W. Singhose, and I. Ebert-Uphoff, "Performance measures for input shaping and command generation," *Journal of Dynamic Systems Measurement and Control*, vol. 78, pp. 731–736, 2006.
- [10] L.-F. Lee, M. Narayanan, F. Mendel, V. Krovi, and P. Karam, "Kinematics analysis of in-parallel 5 dof haptic device," in *2010 IEEE/ASME International Conference on Advanced Intelligent Mechatronics (AIM)*, July 2010, pp. 237–241.
- [11] M. S. Narayanan, S. Kannan, X. Zhou, F. Mendel, and V. Krovi,

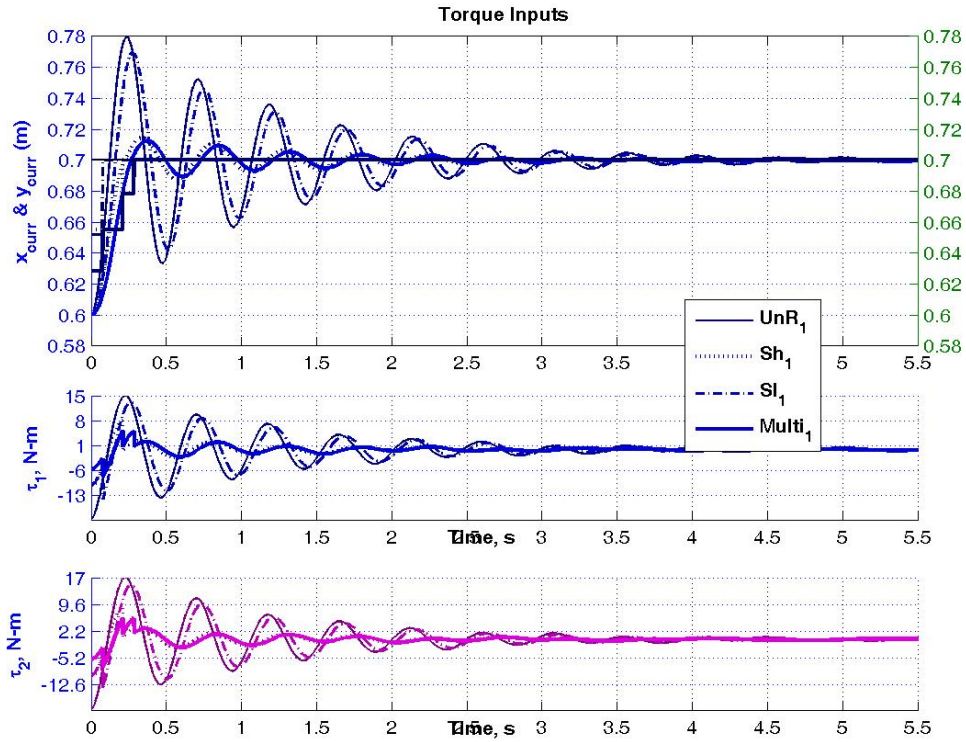


**Fig. 7:** Unshaped and Shaped Responses, and Torque Inputs of 2 –  $\underline{RR}$  PPM based on Mean Value Shaper for Mu-St Test Trajectories

“Parallel architecture for use in masticatory studies,” *International Journal of Intelligent Mechatronics and Robotics (IJIMR)*, vol. 1, no. 4, pp. 100–122, 2012.

#### APPENDIX

##### Dynamic EoM Matrices for 2 – $\underline{RR}$

From Fig.3, it can be noted that the individual chains can be modeled as double pendulum sub-systems with additional loop closure constraint as discussed in eqn.4. Therefore, the mass matrix ( $M$ ), centrifugal-Coriolis ( $H$ ) and input torque ( $U$ ) vectors for a typical double pendulum [8] can be obtained as (use  $i = 1, 2$  for 2 –  $\underline{RR}$  manipulators):

$$M_{DP}^i = \begin{bmatrix} M_{(1,1)}^i & M_{(1,2)}^i \\ M_{(2,1)}^i & M_{(2,2)}^i \end{bmatrix} \quad (12)$$

$$\begin{aligned} \text{where, } M_{(1,1)}^i &= m_{i,1}Lc_{i,1}^2 + m_{i,2}L_{i,2}^2 + J_{i,1} \\ M_{(1,2)}^i &= M_{(2,1)}^i = m_{i,2}L_{i,1}Lc_{i,2}\cos(\theta_i - \phi_i) \\ M_{(2,2)}^i &= m_{i,2}Lc_{i,2}^2 + J_{i,2} \end{aligned}$$

$$H_{DP}^i = \begin{bmatrix} m_{i,2}L_{i,1}Lc_{i,2}\dot{\phi}_i^2\sin(\theta_i - \phi_i) \\ -m_{i,2}L_{i,1}Lc_{i,2}\dot{\theta}_i^2\sin(\theta_i - \phi_i) \end{bmatrix}, U_{DP}^i = \begin{bmatrix} \tau_{i,1} \\ \tau_{i,2} \end{bmatrix} \quad (13)$$

For 2 –  $\underline{RR}$  manipulators, we have:

$$[M_{2RR}]_{4 \times 4} = \text{diag}(M_{DP}^1, M_{DP}^2) + M_{2RR}^{EE} \quad (14)$$

where  $M_{2RR}^{EE}$  is the contribution of end-effector platform mass to the mass-matrix 2 –  $\underline{RR}$  manipulator,

$$\begin{aligned} M_{2RR}^{EE}(1, 1) &= m_p L_{1,1}^2, M_{2RR}^{EE}(2, 2) = m_p L_{1,2}^2 \\ M_{2RR}^{EE}(1, 2) &= M_{2RR}^{EE}(2, 1) = m_p L_{1,1} L_{1,2} \cos(\theta_1 - \phi_1) \end{aligned} \quad (15)$$

$$[H_{2RR}]_{4 \times 1} = [H_{DP}^1, H_{DP}^2] + H_{2RR}^{EE} \quad (16)$$

$$[\tau_{2RR}]_{4 \times 1} = \begin{bmatrix} U_{DP}^1 \\ U_{DP}^2 \end{bmatrix} \quad (17)$$

$$\begin{aligned} H_{2RR}^{EE}(1) &= m_p L_{1,1} L_{1,2} \dot{\phi}_1^2 \sin(\theta_1 - \phi_1) \\ H_{2RR}^{EE}(2) &= -m_p L_{1,1} L_{1,2} \dot{\theta}_1^2 \sin(\theta_1 - \phi_1) \end{aligned} \quad (18)$$

where  $H_{2RR}^{EE}$  is the contribution of end-effector platform mass to the centrifugal and Coriolis force vectors of 2 –  $\underline{RR}$  manipulator.